Carbohydrate Polymers 92 (2013) 1018–1025

Contents lists available at SciVerse ScienceDirect

Carbohydrate Polymers

journal homepage: www.elsevier.com/locate/carbpol

Control of the properties of xanthan/glucomannan mixed gels by varying xanthan fine structure

P. Fitzpatrick[1], J. Meadows[2], I. Ratcliffe, Peter A. Williams*

Centre for Water Soluble Polymers, Glyndwr University, Plas Coch, Mold Road, Wrexham LL11 2AW, UK

ARTICLE INFO

Article history:
Received 25 July 2012
Received in revised form
18 September 2012
Accepted 19 October 2012
Available online 27 October 2012

Keywords:
Konjac glucomannan
Xanthan gum
Thermoreversible gels
DSC
Coil–helix transition

ABSTRACT

The interaction of native xanthan gum, deacetylated xanthan gum and depyruvated xanthan gum with konjac glucomannan has been studied using DSC and controlled stress rheometry. In the absence of electrolyte the DSC cooling curves for native xanthan and deacetylated xanthan showed a single peak and there was a corresponding sharp increase in the storage modulus indicating gel formation. It is apparent that on cooling, association of the konjac glucomannan with the native xanthan molecules is triggered by the xanthan coil–helix transition. In the presence of electrolyte, there were two DSC peaks observed. The higher temperature DSC peak was attributed to the xanthan coil–helix transition while the lower temperature DSC peak was attributed to konjac glucomannan–xanthan association as noted by an increase in the storage modulus. The gels formed were much weaker than those in the absence of electrolyte. The DSC cooling curves for depyruvated xanthan in the absence of electrolyte showed two peaks. The higher temperature peak was attributed to the coil–helix transition while the lower temperature peak corresponded to gelation as noted by an increase in the storage modulus. The gels were very much weaker than for native xanthan gum and deacetylated xanthan gum.

1. Introduction

Xanthan gum is an exocellular polysaccharide produced by the bacterium *Xanthomonas campestris* and is nowadays very widely used in a broad range of products, including foods, pharmaceuticals, cosmetics, personal care, drilling muds, etc. because of its unique rheological properties (Sworn, 2009; Morris, 2006). Essentially, xanthan gum solutions exhibit a very high viscosity at low shear rates because of weak intermolecular association of the polysaccharide chains. However, the solutions are very shear thinning since the weak intermolecular associations are readily disrupted. The gum is, therefore, widely used to stabilise dispersions and emulsions because of its ability to inhibit particle sedimentation and droplet creaming (Velez, Fernandez, Munoz, Williams, & English, 2003). Xanthan molecules consist of a main chain of (1,4)-β-D-glucose residues with a trisaccharide side chain attached to every other glucose. The side chains are linked through the 3 position and consist of β-D-mannose, (1,4)-β-D-glucuronic acid, and (1,2)-α-D-mannose. The inner mannose may be acetylated and the terminal mannose may be pyruvated. Xanthan molecules have been shown by X-ray fibre diffraction studies to adopt a right-handed helical conformation with five-fold symmetry and a pitch of 4.7 nm (Moorhouse, Walkinshaw, & Arnott, 1977). It has been clearly demonstrated by a range of techniques including, optical rotation, viscosity, light scattering, electron microscopy, DSC, NMR and ESR, that the molecules undergo a conformational transition in solution to form a more flexible disordered state which is favoured at increasing temperature and low ionic strength (Foss, Stokke, & Smidsrød, 1987; Gamini, de Bleijser, & Leyte, 1991; Lui & Norisuye, 1988; Milas & Rinaudo, 1986; Norton, Goodall, Frangou, Morris, & Rees, 1984; Takigami, Shimada, Williams, & Phillips, 1993). There is much controversy reported in the literature as to whether the molecules adopt single helices, double helices or dimers through association of single helical chains in solution. For example, Norton et al. (1984) argued that the molecules adopt a single helical conformation with the side chains packed along the backbone and that ordered and disordered sequences may co-exist within the same molecule. Milas and Rinaudo (1986) also favoured the single helix model and suggested that the molecules can adopt three distinct molecular conformations. In the native state, the molecules are completely ordered and on heating become completely disordered. On further cooling the molecules order but are more expanded than the native state as a consequence of different side chain–backbone interactions. On the other hand Lui and Norisuye (1988) concluded that the ordered structure was a double helix and that on increasing

* Corresponding author.
E-mail addresses: paul.fitzpatrick@ctechinnovation.com (P. Fitzpatrick), jmeadows@sinclairpharma.com (J. Meadows), williamspa@glyndwr.ac.uk, p.a.williams@glyndwr.ac.uk (P.A. Williams).
[1] Present address: C-Tech Innovation Ltd., Capenhurst Technology Park, Chester CH1 6EH, UK.
[2] Present address: IS Pharmaceuticals Ltd., Office Village, Chester Business Park, Chester CH4 9QZ, UK.

0144-8617/$ – see front matter © 2012 Elsevier Ltd. All rights reserved.
http://dx.doi.org/10.1016/j.carbpol.2012.10.049

the temperature the molecules unwind from both ends forming an expanded dimer joined by a short helical section. Foss et al. (1987) produced electron micrographs showing that the ordered xanthan consists of two associated molecules with sections of single strands at one or both ends. NMR studies by Gamini et al. (1991) provided support for the expanded dimer concept and also indicated that on heating considerable side chain mobility is established before any significant increase in the mobility of the backbone is observed. In the ordered form the side chains are associated with the cellulosic backbone thus stabilising the helical structure, while in the disordered form there is no association with the backbone and the side chains are free to rotate. Further confirmation of the involvement of the side chains in the ordering process has been provided through ESR studies by Takigami et al. (1993) using nitroxide spin labels attached to the carboxylate groups in the side chains. At high temperatures the side chains were found to be highly mobile giving rise to isotropic ESR spectra but on cooling to temperatures below the conformational transition, anisotropic spectra were obtained indicating a significant loss of mobility. The temperature of the conformational transition is dependent on the amount of acetyl and pyruvate groups present (Callet, Milas, & Rinaudo, 1987; Cheetham & Mashimba, 1992; Shatwell, Sutherland, Dea, & Ross-Murphy, 1990). It has been shown that it shifts to lower temperatures by removal of acetyl groups but increases to higher temperatures on removal of pyruvate groups. The acetyl groups on the side chains are able to interact with the cellulosic backbone through hydrogen or hydrophobic bonding thus promoting the ordered structure. The destabilising effect of the pyruvate groups has been attributed to the increase in electrostatic charge repulsion as a result of the side chains folding in on the backbone.

It is well known that xanthan gum will form thermoreversible gels in the presence of certain galactomannans, namely locust bean gum and tara gum and also with glucomannans (konjac mannan) (Abbaszadeh & Foster, 2012; Annable, Williams, & Nishinari, 1994; Callet et al., 1987; Cheetham & Mashimba, 1992; Dea et al., 1977; Dea & Morrison, 1975; Fitzsimons, Tobin, & Morris, 2008; Wielinga, 2009; Williams, Clegg, Day, Phillips, & Nishinari, 1991; Williams, Day, Langdon, Phillips, & Nishinari, 1991; Williams & Phillips, 1995). The galactomannans consist of linear chains of β-(1,4)-mannose residues with galactose residues linked at the 6 position (Takigami, 2009). The mannose to galactose ratio is 3:1 for tara gum and 4:1 for locust bean gum. Glucomannans consist of linear chains of β-(1,4)-glucose and mannose residues with branches consisting of up to 16 sugar units linked to the 3 position on the main chain (Nishinari, Williams, & Phillips, 1992). There is approximately one branch every 10 residues along the chain. The mannose to glucose ratio is 1.6:1. The molecules also contain acetyl groups (approximately 1 per 17 sugar residues). A common feature of galactomannans and glucomannans with respect to their interaction with xanthan gum is that they adopt an extended conformation in solution. The thermoreversible gels formed by mixing xanthan gum with tara gum, locust bean gum or konjac glucomannan are optically clear and highly elastic and have considerable commercial importance. The mechanism of the gelation process has been a matter of much controversy and a detailed review has been published previously (Williams & Phillips, 1995). It is clear that the main body of evidence indicates that gelation occurs as a consequence of the molecular association of xanthan molecules with galacto- and gluco-mannan chains. Brownsey, Cairns, Miles, & Morris (1988) studied the mixed systems using X-ray diffraction and the X-ray fibre pattern obtained provided direct evidence of intermolecular binding. Since gels were only formed when solutions were mixed at temperatures above the xanthan coil–helix transition, binding was assumed to involve the disordered xanthan chains. Dea and Morrison (1975), however, proposed that association involved the ordered xanthan helices. More recent work by Fitzsimons et al. (2008) provides further evidence that the association does not require xanthan to be in the disordered form. These workers, however, demonstrated that stronger gels are formed after heating to 95 °C [i.e. above the temperature of the coil helix transition] and then cooling to 20 °C than those obtained on mixing at 20 °C. This is in agreement with our own previous work using a combination of DSC, rheology and ESR techniques which demonstrated that the molecular association between xanthan and galacto- and gluco-mannans only occurs at temperatures at or below the xanthan conformational transition (Annable et al., 1994; Williams & Phillips, 1995; Williams, Day, et al., 1991). A number of workers (Abbaszadeh & Foster, 2012; Shatwell, Sutherland, Ross-Murphy, & Dea, 1991; Tako, Asato, & Nakamura, 1984) have shown that the interaction of xanthan with galacto- and gluco-mannans is dependent of the degree of acetylation and pyruvation of the xanthan molecules. Deacetylated xanthan has been found to produce much stronger gels than native or depyruvated xanthan molecules. This study sets out to gain a further insight into the mechanism of gelation of konjac glucomannan/xanthan gum mixed systems using xanthan, deaceylated xanthan and depyruvated xanthan with a view to controlling the thermal and rheological properties of the mixed gels.

2. Materials and methods

2.1. Xanthan gum

A commercial sample of xanthan gum was dialysed against deionised water and the metal ion content determined using Atomic Absorption. It was found to contain 0.021% Na, 0.029% K and 0.002% Ca. The acetyl content was determined by alkaline hydrolysis as follows: Nitrogen gas was passed through 100 mL 0.5% (w/w) xanthan solution for 10 min and 3 mL of 1 M KOH added. The flask was stoppered and left for 2 days at room temperature with intermittent stirring. 30 mL 0.05 H_2SO_4 was added and the excess acid was titrated with 0.01 M KOH using phenolphthalein indicator. It was found that 93% of the side chains were acetylated. The pyruvate content was determined using the method reported by Sloneker and Orentas (1962) and it was found that 25% of the side chains contained a pyruvate group.

2.2. Deacetylated xanthan gum

The commercial sample reported above was deacetylated using the method described by Tako and Nakamura (1984).

2.3. Depyruvated xanthan gum

A sample of depyruvated xanthan was provided as a gift and it was found that 90% of the side chains were acetylated and 7% contained a pyruvate group.

2.4. Konjac glucomannan (KM)

A commercial sample of hydroprocessed konjac glucomannan was obtained and was used as received. It was found to contain negligible amounts of metal ions and had a molecular mass of 480 kDa and acetyl content of 1 per 17 sugar units.

2.5. Differential scanning calorimetry

Measurements were performed using a Seteram micro DSC fitted with 1 mL sample vessels. The polymer solution was accurately weighed into the sample cell and the reference cell was filled with the same weight of solvent. Instrumental baselines were determined with both the sample and reference cells filled with solvent

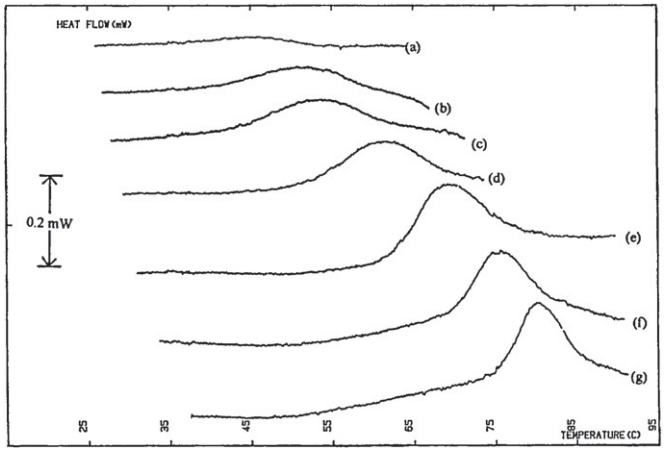

Fig. 1. DSC cooling curves for 1.2% native xanthan gum solution in (a) water, (b) 5 mM, (c) 8 mM, (d) 10 mM, (e) 20 mM, (f) 30 mM and (g) 40 mM NaCl.

and the curve produced was subtracted from the sample curve. The scans were determined at a scan rate of 0.2 °C/min and an initial heat/cool cycle was undertaken to ensure the same thermal history.

2.6. Rheological measurements

Rheological experiments were performed on a Carrimed CSL 100 Controlled Stress Rheometer using cone and plate geometry (2° × 5 cm). Samples were prepared in the presence and absence of electrolyte and heated to 75 °C then loaded onto the instrument. They were then cooled at a constant rate of 1 °C/min in 5 °C steps. The storage (G') and loss (G'') moduli were determined at each step at a frequency of 1 Hz down to 15 °C. A 3 min equilibration step was allowed at each interval.

3. Results and discussion

3.1. Xanthan conformational transition

The DSC cooling curves for native xanthan gum solutions (1.2%, w/w) at different ionic strengths are given in Fig. 1. The cooling curve in the absence of electrolyte (curve a) shows a very broad exothermic peak between ~35 and 55 °C which is not readily discernible. This indicates that the conformational transition occurs over a large temperature range and has a very small enthalpy. This is presumably due to the fact the charged carboxylate groups present on the xanthan side chains inhibit them from folding onto the xanthan backbone due to electrostatic repulsions and hence the molecules adopt a less ordered structure. In the presence of 5 mM NaCl (curve b) a small exothermic peak is observed with a midpoint transition temperature, T_m, of 52.1 °C which is attributed to the xanthan coil–helix transition. As the ionic strength is increased (curves c–g) the peak shifts to higher temperatures and becomes much sharper. The presence of the electrolyte will screen electrostatic repulsions between the charged groups on the side-chains enabling them to fold in and bind to the xanthan backbone and stabilise the helical structure. The xanthan molecules, therefore, undergo the coil–helix transition at a higher temperature and the molecules have a greater degree of order. The values for the midpoint transition temperature, T_m, and the enthalpy of the process, ΔH, are summarised in Table 1. It is noted that the enthalpy increases from −2.6 J/g in 1 mM NaCl up to −6.5 J/g in 20 mM NaCl and then remains constant. This latter value is in good agreement with Fitzsimons et al. (2008) who reported a value of −6.00 J/g in 30 mM KCl. Kitamura, Takeo, Kuge, and Stokke (1991) also showed that ΔH was independent of electrolyte concentration above 20 mM NaCl but the actual value obtained was slightly higher than for our sample (8.6 J/g).

Table 1
Enthalpy and transition midpoint temperatures as a function of ionic strength for native xanthan and deacetylated xanthan on cooling.

Ionic strength (mM)	Native xanthan		Deacetylated xanthan	
	T_m	ΔH (J/g)	T_m	ΔH (J/g)
1	51.4	−2.6		
5	52.1	−2.7		
8	53.7	−3.3		
10	61.0	−5.2	45.8	−2.5
15	65.2	−5.6		
20	69.1	−6.6	56.7	−4.2
25	73.0	−6.5		
30	75.2	−6.3	62.6	−4.1
35	76.5	−6.5		
40	80.3	−6.5	66.8	−4.0

The corresponding DSC cooling curves for deacetylated xanthan gum solutions (1.2%, w/w) at different ionic strengths are presented in Fig. 2. It is evident that the conformational transition occurs at a lower temperature compared to xanthan itself at the various ionic strengths. The T_m values of the transition and the ΔH values are summarised in Table 1. The ΔH values follow a similar trend as for the standard xanthan sample in that they increase up to 20 mM NaCl and then remain constant. However, the actual values (−4.2 J/g) are considerably lower for the deacetylated sample compared to the native xanthan. Presumably, the lower ΔH and T_m values are a consequence of the fact that when acetyl groups are removed from the mannose residues on the side chains, the side chains are no longer able to associate with the backbone as effectively and, therefore, are not able to stabilise the helical structure. Hence, lower temperatures are required for the coil–helix transition to occur and the molecules adopt a less stable structure.

According to the Manning theory for polyelectrolytes (Manning, 1969a, 1969b, 1996), counterion condensation will occur when the dimensionless linear charge density parameter, ξ, has a value greater than Z^{-1}, where Z is the valency of the counterion. ξ can be calculated using the relationship,

$$\xi = \frac{e^2}{4\pi\varepsilon_o\varepsilon\kappa Tb} \quad (1)$$

where e is electronic charge, ε_o and ε are the permittivity in vacuum and in the solvent, κ, is the Boltzmann constant, T, is the absolute

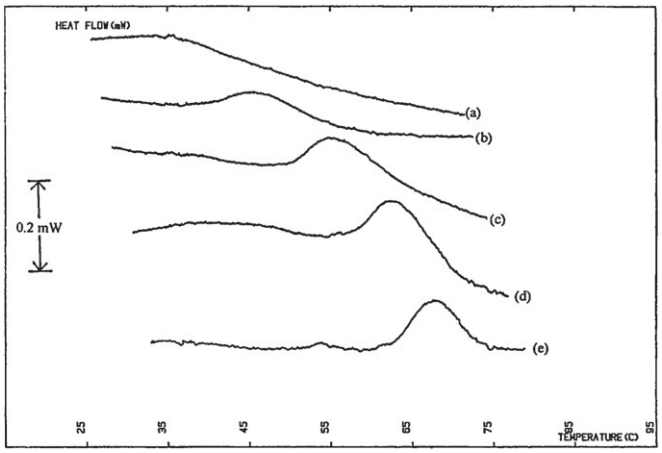

Fig. 2. DSC cooling curves for deacetylated xanthan gum (1.2%) in (a) water, (b) 10 mM, (c) 20 mM, (d) 30 mM and (e) 40 mM NaCl.

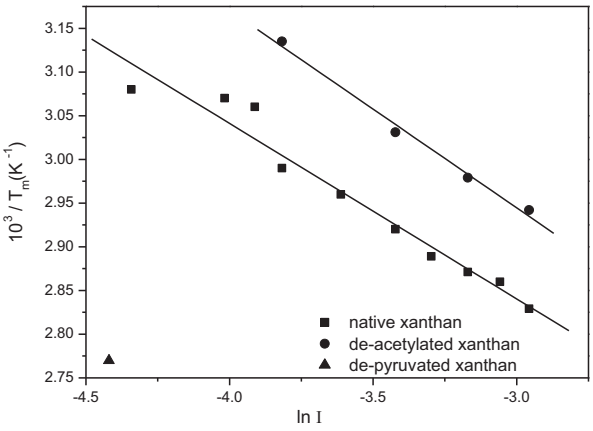

Fig. 3. Plot of the inverse of the midpoint transition temperature with the natural log of the ionic strength for native xanthan gum, deacetylated xanthan gum and depyruvated xanthan gum solutions.

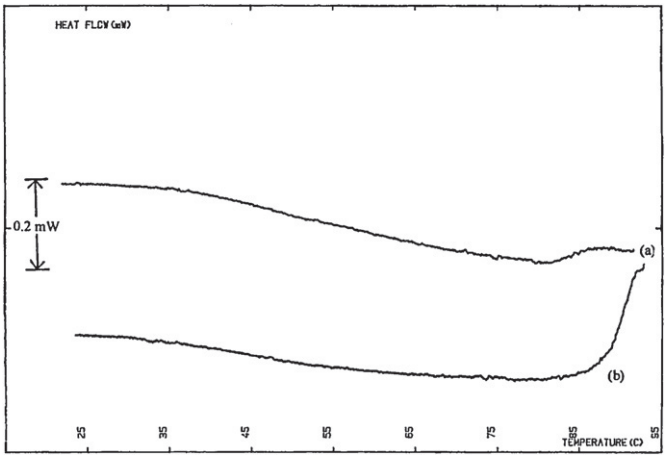

Fig. 4. DSC cooling curves for depyruvated xanthan (1.2%, w/w) in (a) water and (b) 40 mM NaCl.

temperature and *b*, is the spacing between charged groups along the polymer chain.

The fraction of polymer charges carrying a bound counterion, θ, is given by,

$$\theta = Z^{-1}\left[1 - \frac{1}{Z\xi}\right] \quad (2)$$

Norton et al. (1984) carried out DSC studies on a sample of xanthan with an average of 0.67 pyruvate groups per side chain and, therefore, assumed an average of 1.67 charges per xanthan pentasaccharide in order to calculate '*b*'. This is perhaps an oversimplification of the situation since the calculation should strictly have taken into account the distance between the charged pyruvate and glucuronic acid groups on a single side chain and the distance between charged groups on different side chains rather than the average. Nevertheless, they calculated the distance of separation of the charges along the xanthan chain, *b*, to be 0.563 nm for a single stranded chain and 0.281 nm for a double stranded chain yielding values for θ of 0.21 for a single helix and 0.61 for a double helix. The helix–coil transition, therefore, should be accompanied by an increase in the degree of counterion condensation. The extent of increased condensation can be determined using the relationship,

$$\frac{1}{T_m} = \frac{-\theta R \ln I}{2\Delta H_c + \text{constant}} \quad (3)$$

where I is the ionic strength and ΔH_c is the enthalpy change per charge for helix melting.

The inverse transition midpoint temperatures for our samples are plotted as a function of the natural logarithm of the ionic strength (counterions to the polymer plus added NaCl) in Fig. 3. The plots are linear as observed by other workers (Norton et al., 1984; Abbaszadeh & Foster, 2012; Kitamura et al., 1991) in agreement with predictions from Eq. (3). The slope of the line was found to be -0.22×10^{-3} and -0.20×10^{-3} for native xanthan and deacetylated xanthan respectively. These values are close to the value of -0.17×10^{-3} reported by Norton et al. (1984). They used this value to calculate the change in the fraction of charged groups carrying a condensed counterion, $\Delta\theta$, and obtained a value of 0.17. Not withstanding the comments above, this value is close to the value of 0.12 predicted by Manning theory for a coil to single helix transition and significantly less than the value of 0.52 for double helix formation.

Experiments were also undertaken using depyruvated xanthan gum in water and 40 mM NaCl and the DSC cooling curves are presented in Fig. 4. A small exothermic peak can be observed at ~85 °C in water which appears to become more pronounced in the presence of electrolyte. The removal of pyruvate groups from the end of the side chains is expected to facilitate formation of the ordered structure since it reduces electrostatic repulsions and hence the conformational transition shifts to higher temperatures.

3.2. Xanthan/KM mixed systems in the absence of electrolyte

The DSC cooling curves for native xanthan and deacetylated xanthan in the presence of konjac glucomannan (1:1 mixing ratio; 1.2% total polysaccharide, w/w) are given in Fig. 5. The native xanthan/konjac glucomannan (curve a) and deacetylated xanthan/konjac glucomannan (curve b) show a single peak with onset temperatures of 64 °C and 59 °C, respectively. The corresponding G' and G'' values of these systems were measured at 1 Hz on cooling over the same temperature range and the results are presented in Fig. 6. G' is seen to increase at ~64 °C and 59 °C for the native xanthan and deacetylated xanthan, respectively. These temperatures correspond closely with the onset temperature of the conformational transition of the respective samples (Fig. 5). The implication is that konjac glucomannan molecules associate strongly with the xanthan molecules once the ordering process has started resulting in the formation of a three dimensional gel structure as reported previously (Annable et al., 1994). Our key conclusion is that for these systems, in the absence of electrolyte, the coil–helix transition is the trigger for the interaction to occur. This contradicts the work of Cairns, Miles, and Morris (1986) and Brownsey et al. (1988)

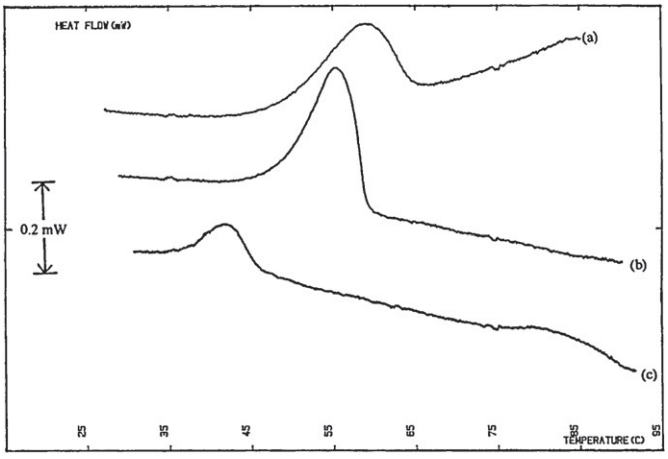

Fig. 5. DSC cooling curves for (a) native xanthan gum, (b) deacetylated xanthan gum and (c) depyruvated xanthan in admixture with KM (1:1 mixing ratio; 1.2% total polysaccharide).

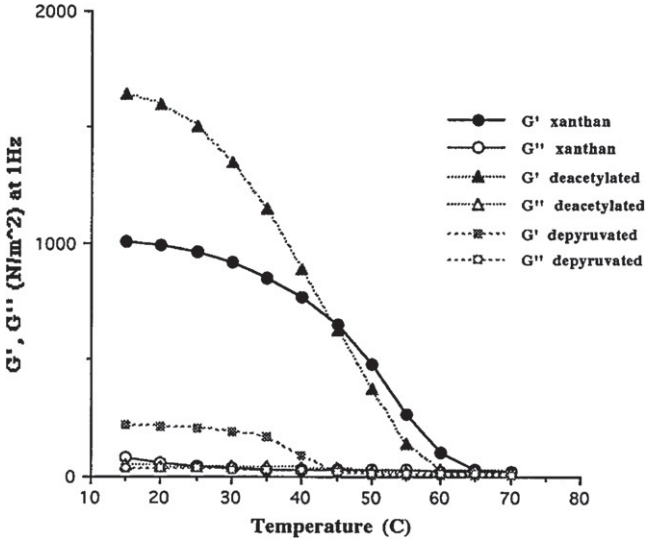

Fig. 6. Variation of G' and G'' at 1 Hz of xanthan/KM samples [mixing ratio 1:1; 1.2% total polysaccharide] on cooling.

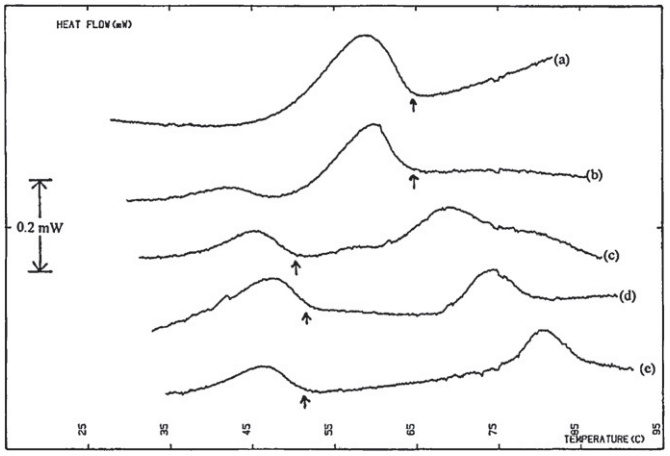

Fig. 7. DSC cooling curves for native xanthan gum/KM solutions (1:1 mixing ratio; 1.2% total polysaccharide) in (a) water, (b) 10 mM, (c) 20 mM, (d) 30 mM, and (e) 40 mM NaCl. The arrows show the temperature of gelation.

who indicated that binding occurred only with disordered xanthan chains and also with Goycoolea, Richardson, Morris, & Gidley (1995) who argued that the interaction can occur with both ordered and disordered chains. Our results indicate that the mechanism of interaction is similar to that for mixtures of konjac glucomannan with kappa carrageenan (Williams, Clegg, Langdon, Nishinari, & Piculell, 1993) in which molecular association and gelation occur only once the carrageenan molecules form the ordered helical structure. We have demonstrated previously by ESR nitroxide spin labelling studies that the segmental motion of the konjac glucomannan molecules decreases dramatically as the xanthan molecules form the ordered structure and this can only be attributed to association of the konjac glucomannan with xanthan molecules (Annable et al., 1994). The values of G' at 20 °C and at 1 Hz are 1600 Nm^{-2} and 1000 Nm^{-2} for the deacetylated and unmodified xanthan samples respectively. Other workers, (Abbaszadeh & Foster, 2012; Shatwell et al., 1991; Tako et al., 1984) have also reported higher G' values for deacetylated xanthan.

The DSC cooling curves for depyruvated xanthan/konjac glucomannan (1:1 mixing ratio; 1.2% total polysaccharide, w/w) are also presented in Fig. 5 curve (c). For this sample two peaks were observed one with an onset temperature at 85 °C and the other at 45 °C. The corresponding G' and G'' values of this system were measured at 1 Hz on cooling over the same temperature range and the results are also presented in Fig. 6. G' is seen to increase at ~45 °C although the maximum value attained is considerably lower than for the xanthan and deacetylated xanthan systems. The high temperature DSC peak is attributed to the ordering of the xanthan chains while the peak at lower temperature corresponds to the temperature of gelation. In the case of depyruvated xanthan, the molecules are already ordered at the start of the rheological measurements (75 °C) and molecular association with konjac glucomannan molecules occurs at a lower temperature.

The ΔH values for the DSC peaks were found to be −8.4 J/g, −11.3 J/g and −2.6 J/g, respectively, for the native xanthan, deacetylated xanthan and depyruvated xanthan mixtures respectively (Table 2). These values are considerably higher than for the respective xanthan samples alone supporting the concept that konjac glucomannan associates with the xanthan molecules promoting the formation of the ordered structure which leads to the formation of a three dimensional gel network. It is noteworthy that the enthalpy value is highest for the deacetylated sample which is expected to have the least ordered helical structure and lowest for the depyruvated sample which is expected to have the most ordered helical structure.

3.3. Xanthan/KM mixed systems in the presence of electrolyte

The DSC cooling curves and corresponding G' and G'' values at 1 Hz for native xanthan/konjac glucomannan mixtures (1:1 mixing ratio; 1.2% total polysaccharide) at varying ionic strength are given in Figs. 7 and 8. In the absence of electrolyte a single large exothermic peak is observed by DSC with an onset temperature of ~64 °C corresponding to the gelation temperature as noted by the increase in G' (Fig. 8). In the presence of 10 mM NaCl a similar peak is observed with an onset temperature of 64 °C again corresponding to the temperature of gelation (Fig. 8). There is also a small DSC peak with an onset temperature at ~47 °C. As the ionic strength is increased further to 20 mM, 30 mM and 40 mM NaCl (curves c–e) two exothermic peaks are observed by DSC. The enthalpies for all of the peaks are given in Table 2. The peaks at higher temperature have onset temperatures of 70-85 °C similar to the peaks observed previously for the xanthan alone. We, therefore, attribute these peaks to the xanthan conformational transition. The peaks at lower

Table 2
Enthalpy and onset temperatures as a function of ionic strength for natuve xanthan, deacetylated xanthan and depyruvated xanthan in admixture with KM on cooling.

Ionic strength (mM)	Native xanthan/KM ΔH (J/g)		Deacetylated xanthan/KM ΔH (J/g)		Depyruvated xanthan/KM ΔH (J/g)	
	Peak onset ~64 °C	Peak onset ~50 °C	Peak onset ~59 °C	Peak onset ~54 °C	Peak onset ~50 °C	Peak onset ~45 °C
Water	−8.38		−11.28			−2.63
10	−4.67	−0.79	−10.79			
20		−2.12	−2.60	−2.52		
30		−2.88		−4.38		
40		−2.25		−4.43	−2.13	

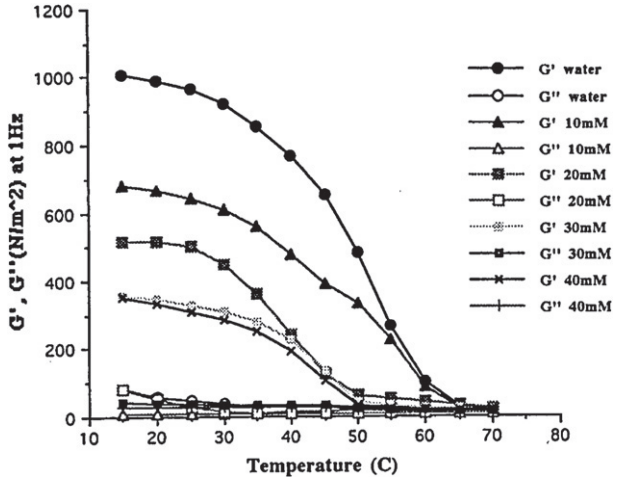

Fig. 8. Variation of G' and G'' at 1 Hz on cooling for native xanthan gum/KM solutions (1:1 mixing ratio; 1.2% total polysaccharide) at different ionic strengths.

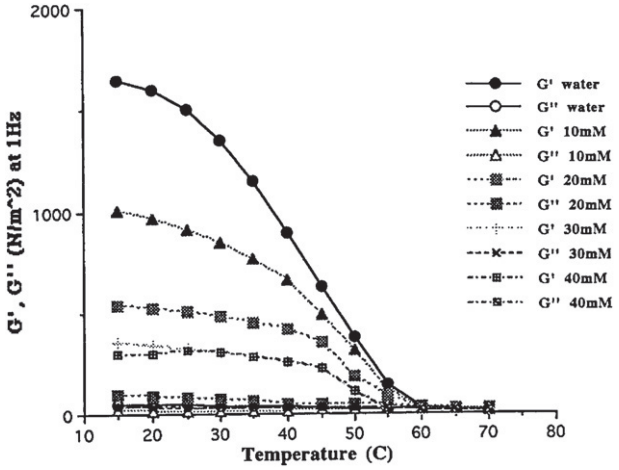

Fig. 10. Variation of G' and G'' at 1 Hz on cooling for deacetylated xanthan/KM (1:1 mixing ratio, 1.2% total polysaccharide concentration at different ionic strengths.

temperatures have onset temperatures at ~52 °C which corresponds to the gelation temperatures as noted by the increase in G' (Fig. 8). It is evident that the value of G' decreases in the presence of electrolyte from 1000 Nm^{-2} in water to 350 Nm^{-2} in 40 mM NaCl. The lower value for G' and the lower enthalpy values associated with this peak are indicative of a less extensive interaction between the xanthan and konjac glucomannan molecules.

Similar experiments were undertaken using deacetylated xanthan and the DSC cooling curves and enthalpy values are given in Fig. 9 and Table 2 and the corresponding G' and G'' values are presented in Fig. 10. For the systems in water and 10 mM NaCl a large exothermic DSC peak is observed with an onset temperature of ~60 °C which corresponds to the temperature of gelation. In the presence of 20 mM NaCl (curve c) two exothermic peaks are observed. The peak with T_m at 57 °C has a shoulder on the high temperature side, which has the same onset temperature as for the conformational transition of deacetylated xanthan itself (Fig. 2). The peak corresponds to the temperature of gelation as noted by the increase in the value of G' at ~60 °C as shown in Fig. 10. The lower temperature peak with a T_m ~50 °C is also due to molecular aggregation as noted by a shoulder in the plot of G' against temperature. In the presence of 30 and 40 mM NaCl two peaks are observed. The higher temperature peak corresponds to the xanthan conformational transition as reported above (Fig. 2) while the lower temperature peak with an onset temperature of 54 °C corresponds to the increase in G' as a result of xanthan/konjac glucomannan molecular association. The value of G' decreases from 1600 Nm^{-2} in water to 250 Nm^{-2} in the presence of 40 mM NaCl. The lower G' values and lower enthalpies obtained in the presence of electrolyte are again indicative of a less extensive interaction between the deacetylated xanthan and konjac glucomannan molecules.

The DSC cooling curves, enthalpy values and corresponding G' and G'' values for depyruvated xanthan/konjac glucomannan mixtures in water and 40 mM NaCl (1:1 mixing ratio; 1.2% total polysaccharide) are shown in Table 2 and Figs. 11 and 12. The DSC cooling curve in water (Fig. 11 curve a) shows a small exothermic peak with T_m ~80 °C which corresponds to the xanthan conformational transition and a second peak with an onset temperature of ~45 °C. This lower temperature peak corresponds to gelation as noted by the increase in G' (Fig. 12). In the presence of 40 mM NaCl (Fig. 11 curve b) there is only one peak observed. It is expected that the peak due to the xanthan conformational transition is >90 °C and that the peak observed with an onset temperature of ~50 °C corresponds to the increase in G' and the onset of gelation (Fig. 12). For depyruvated xanthan the values for G' are very much less than for the standard and deacetylated xanthan samples and contrary to these samples G' increases slightly in the presence of electrolyte.

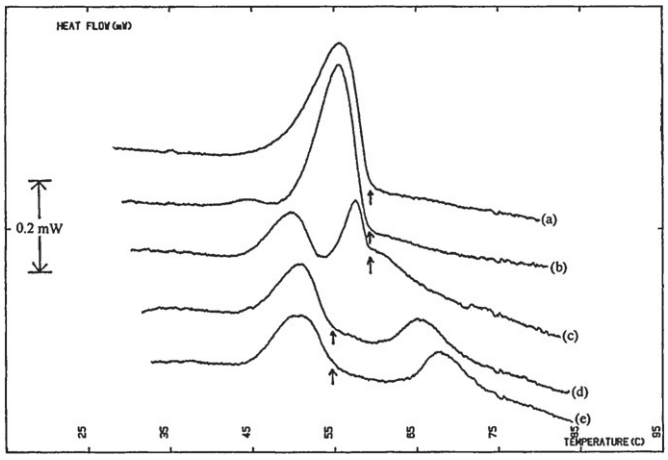

Fig. 9. DSC cooling curves for deacetylated xanthan/KM (1:1 mixture: total polysaccharide concentration 1.2%) in (a) water, (b) 10 mM, (c) 20 mM, (d) 30 mM, and (e) 40 mM NaCl. The arrows show the temperature of gelation.

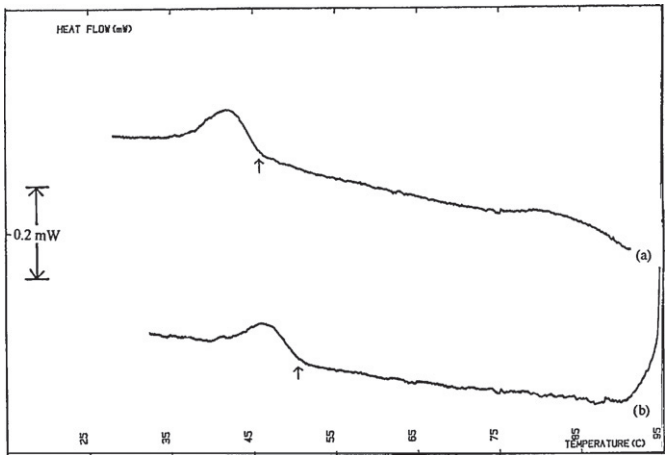

Fig. 11. DSC cooling curves for depyruvated xanthan/KM solutions (1:1 mixture; 1.2% total polysaccharide) in (a) water and (b) 40 mM NaCl.

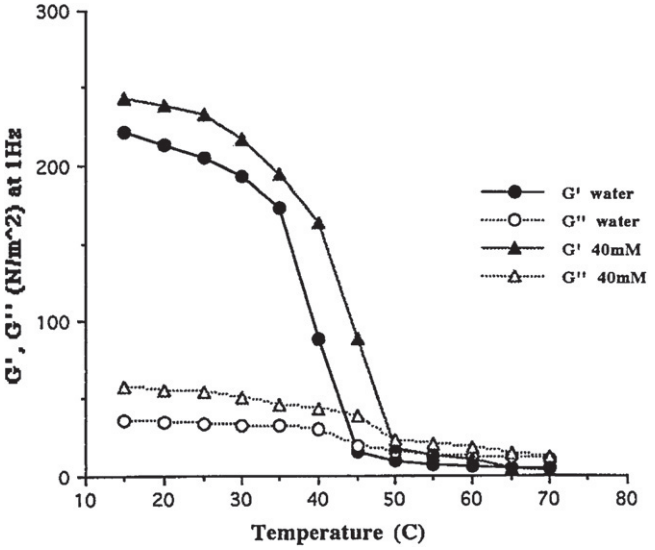

Fig. 12. Variation of G' and G'' at 1Hx on cooling for depyruvated xanthan/KM mixtures (1:1 mixing ratio; 1.2% total polysaccharide) in water and 40 mM NaCl.

In water at 20 C, G' has a value of 210 Nm^{-2} while in 40 mM NaCl it increases to 240 Nm^{-2}.

4. Conclusions

In summary it is noted that xanthan gum forms thermoreversible gels with konjac glucomannan as a result of molecular association. The gels are stronger in water than in the presence of electrolyte and gel strength decreases in the order deacetylated xanthan/konjac glucomannan > xanthan/konjac glucomannan ≫ depyruvated xanthan/konjac glucomannan.

For native xanthan and deacetylated xanthan mixtures with konjac glucomannan in water the xanthan conformational transition and gelation are coincidental. It appears that as the xanthan molecules order they associate with konjac glucomannan molecules resulting in the formation of a three-dimensional gel network. The significantly higher enthalpies obtained for the mixed systems demonstrate that the degree of molecular ordering is greater than for xanthan alone. In addition, the degree of ordering is less for deacetylated xanthan than native xanthan in the absence of konjac glucomannan and it is interesting to note that this results in the deacetylated xanthan having higher enthalpy and G' values indicating increased association between xanthan and konjac glucomannan molecules.

For native xanthan and deacetylated xanthan in the presence of electrolyte (>20 mM) the xanthan molecules undergo a coil–helix transition at higher temperatures than in water but interaction with konjac glucomannan molecules only occurs at much lower temperatures. This is presumably due to the increased thermal energy of the molecules at high temperature, which inhibits molecular association. As the temperature decreases, xanthan/konjac glucomannan association and gelation occurs but to a lesser extent than in the absence of electrolyte as indicated by the lower enthalpies and G' values. We conclude that in these systems self-association of xanthan molecules competes with xanthan/konjac glucomannan association due to charge screening by the electrolyte present.

The depyruvated xanthan forms an ordered structure at high temperatures even in the absence of electrolyte and association with konjac glucomannan molecules is much less than for standard and deacetylated xanthan as confirmed by the DSC and rheological measurements.

References

Abbaszadeh, A., & Foster, T. J. (2012). Effect of polymer fine structure on synergistic interactions of xanthan with konjac glucomannan. In P. A. Williams, & G. O. Phillips (Eds.), *Gums and stabilisers for the food industry* (p. 151). Cambridge, UK: RSC Publishing. Special Publication No. 335.

Annable, P., Williams, P. A., & Nishinari, K. (1994). Interaction in xanthan–glucomannan mixtures and the effect of electrolyte. *Macromolecules*, *27*, 4204.

Brownsey, G. J., Cairns, P., Miles, M. J., & Morris, V. J. (1988). Evidence for intermolecular binding between xanthan and the glucomannan konjac mannan. *Carbohydrate Research*, *176*, 329.

Cairns, P., Miles, M. J., & Morris, V. J. (1986). *Intermolecular bonding of xanthan gum and carob gum*, *322*, 89–90.

Callet, F., Milas, M., & Rinaudo, M. (1987). Influence of acetyl and pyruvate contents on rheological properties of xanthan in dilute solution. *International Journal of Biological Macromolecules*, *9*, 291–293.

Cheetham, N. W. H., & Mashimba, E. N. M. (1992). Conformational aspects of xanthan–galactomannan gelation. Further evidence from optical-rotation studies. *Carbohydrate Polymers*, *14*, 17.

Dea, I. C. M., Morris, E. R., Rees, D. A., Welsh, E. J., Barnes, H. A., & Price, J. (1977). Associations of like and unlike polysaccharides: Mechanism and specificity in galctomannans, interacting bacterial polysaccharides, and related systems. *Carbohydrate Research*, *57*, 249–272.

Dea, I. C. M., & Morrison, A. (1975). Chemistry and interaction of seed galactomannans. *Advances in Carbohydrate Chemistry and Biochemistry*, *31*, 241.

Fitzsimons, S. M., Tobin, J. T., & Morris, E. R. (2008). Synergistic binding of konjac glucomannan to xanthan on mixing at room temperature. *Food Hydrocolloids*, *22*, 36–46.

Foss, P., Stokke, B. T., & Smidsrød, O. (1987). Thermal stability and chain conformational studies of xanthan at different ionic strengths. *Carbohydrate Polymers*, *7*, 421–433.

Gamini, A., de Bleijser, J., & Leyte, J. C. (1991). Physico-chemical properties of aqueous solutions of xanthan: An NMR study. *Carbohydrate Research*, *220*, 33–47.

Goycoolea, F. M., Richardson, R. K., Morris, E. R., & Gidley, M. J. (1995). Stoichiometry and conformation of xanthan in synergistic gels with locust bean gum or konjac glucomannan: Evidence of heterotypic binding. *Macromolecules*, *28*, 8308–8320.

Kitamura, S., Takeo, K., Kuge, T., & Stokke, B. T. (1991). Thermally induced conformational transition of double stranded xanthan in aqueous solution. *Biopolymers*, *31*, 1243–1255.

Lui, W., & Norisuye, T. (1988). Thermally induced conformational change of xanthan: Interpretation of viscosity behaviour in 0.01 M aqueous sodium chloride. *International Journal of Biological Macromolecules*, *10*, 44.

Manning, G. S. (1969a). Limiting laws and counterion condensation in polyelectrolyte solutions. I. Colligative properties. *Journal Chemical Physics*, *51*, 924–933.

Manning, G. S. (1969b). Limiting laws and counterion condensation in poplyelectrolyte solutions. III. An analysis based on Mayer ionic solution theory. *Journal of Chemical Physics*, *51*, 3249–3252.

Manning, G. S. (1996). Critical onset counterion condensation. A survey if its experimental and theoretical basis. *Berichte der Bunsengesellschaft für physikalische Chemie*, *100*, 909–922.

Milas, M., & Rinaudo, M. (1986). Properties of xanthan gum in aqueous solutions: Role of the conformational transition. *Carbohydrate Research*, *158*, 191.

Moorhouse, R., Walkinshaw, M. D., & Arnott, S. (1977). *ACS Symposium Series*, *45*, 90–102.

Morris, V. J. (2006). Bacterial polysaccharides. In A. M. Stephen, G. O. Phillips, & P. A. Williams (Eds.), *Food polysaccharides and their applications* (2nd ed., vol. 16, pp. 413–454). Boca Raton, FL, USA: CRC Press, Taylor and Francis Group.

Nishinari, K., Williams, P. A., & Phillips, G. O. (1992). Review of the physicochemical characteristics and properties of konjac mannan. *Food Hydrocolloids*, *6*, 199–222.

Norton, I. T., Goodall, D. M., Frangou, S. A., Morris, E. R., & Rees, D. A. (1984). Mechanism and dynamics of conformational ordering in xanthan polysaccharide. *Journal of Molecular Biology*, *175*, 371–394.

Shatwell, K. P., Sutherland, I. W., Dea, I. C. M., & Ross-Murphy, S. B. (1990). The influence of acetyl and pyruvate substituents on the coil–helix transition behaviour of xanthan. *Carbohydrate Research*, *206*, 87–103.

Shatwell, K. P., Sutherland, I. W., Ross-Murphy, S. B., & Dea, I. C. M. (1991). Influence of the acetyl substituent on the interaction of xanthan with plant polysaccharides – III. Xanthan–konjac mannan systems. *Carbohydrate Polymers*, *14*, 131–147.

Sloneker, J. H., & Orentas, D. G. (1962). Pyruvic acid, a unique component of an exocellular bacterial polysaccharide. *Nature*, *194*, 478–479.

Sworn, G. (2009). Xanthan gum. In G. O. Phillips, & P. A. Williams (Eds.), *Handbook of hydrocolloids* (p. 186). Cambridge, UK: CRC Press, Woodhead Publishing Ltd.

Tako, M., Asato, A., & Nakamura, S. (1984). Rheological aspects of the intermolecular interaction between xanthan and locust bean gum in aqueous media. *Agricultural and Biological Chemistry*, *12*, 2995–3000.

Tako, M., & Nakamura, S. (1984). Rheological properties of deacetylated xanthan in aqueous solution. *Agricultural and Biological Chemistry*, *48*, 2987–2993.

Takigami, S. (2009). Konjac mannan. In G. O. Phillips, & P. A. Williams (Eds.), *Handbook of hydrocolloids* (p. 889). Cambridge, UK: CRC Press, Woodhead Publishing Ltd.

Takigami, S., Shimada, M., Williams, P. A., & Phillips, G. O. (1993). ESR study of the conformational transition of spin-labelled xanthan gum in aqueous solution. *International Journal of Biological Macromolecules*, *15*, 367–371.

Velez, G., Fernandez, M. A., Munoz, J., Williams, P. A., & English, R. J. (2003). The role of hydrocolloids on the creaming of oil-in-water emulsions. *Journal of Agricultural & Food Chemistry*, *51*, 265–269.

Wielinga, W. C. (2009). Galactomannans. In G. O. Phillips, & P. A. Williams (Eds.), *Handbook of hydrocolloids* (p. 228). Cambridge, UK: CRC Press, Woodhead Publishing Ltd.

Williams, P. A., Clegg, S. M., Day, D. H., Phillips, G. O., & Nishinari, K. (1991). Mixed gels formed with konjac mannan and xanthan gum. In E. Dickinson (Ed.), *Food polymers, gels and colloids* (p. 339). Cambridge: RSC Special Publication No. 82.

Williams, P. A., Clegg, S. M., Langdon, M. J., Nishinari, K., & Piculell, L. (1993). Investigation of kappa carrageenan/konjac mannan mixed gels by differential scanning calorimetry and electron spin resonance spectroscopy. *Macromolecules*, *26*, 5441–5446.

Williams, P. A., Day, D. H., Langdon, M. J., Phillips, G. O., & Nishinari, K. (1991). Synergistic interaction of xanthan with gluco- and galacto-mannans. *Food Hydrocollolloids*, *4*, 489–493.

Williams, P. A., & Phillips, G. O. (1995). Interactions in mixed polysaccharide systems. In A. M. Stephen (Ed.), *Food polysaccharides and their applications* (p. 463). New York: Marcel Dekker Inc.